


Chapter 23

Fluorinated Oligoazomethine with Azo Groups in the Main Chain as Stimuli-Responsive Photoactive Materials



Yu. Kurioz , I. Tkachenko, A. Kovalchuk, Ya. Kobzar, O. Shekera, R. Kravchuk, V. Nazarenko, and V. Shevchenko

23.1 Introduction

Stimuli-responsive polymers based on photochromic switches (azobenzenes, diarylethenes, spiropyrans, azomethines) have attracted increasing attention due to their possible use in data storage devices, sensors, molecular switches, studies of surface phenomena, etc. [1–6]. Among different photoactive units, azo and azomethine (imine) groups are considered as highly efficient ones and, therefore, great attention has been paid to the synthesis of polyazobenzenes [7–10] and polyazomethines [10–13]. It is important to highlight that the energy levels of the HOMO and LUMO of the molecule bearing the $N = N$ or $CH = N$ double bonds are lower than that of the $C = C$ analog. In fact, the HOMO and LUMO energy levels and energy gaps directly influence on optical properties of corresponding materials [10, 14, 15]. Generally, structures and functional optical properties (reversible *trans-cis* isomerization, photoinduced birefringence, photoluminescence, photovoltaic, etc.) of these polymers are well documented in the literature [1–21]. In addition to distinct optical properties, many studies have been dedicated to the synthesis of chelating agents based on polyazobenzenes (azobenzenes) and, especially, polyazomethines (azomethines) [22–24].

The introduction of novel and unique conjugated fragments into polymer main chains is an important way to realize superior properties from the final products

Yu. Kurioz (✉) · R. Kravchuk · V. Nazarenko

Institute of Physics, National Academy of Sciences of Ukraine, Prospect Nauky 46, Kyiv 03028, Ukraine

e-mail: kurioz@hotmail.com

I. Tkachenko · A. Kovalchuk · Ya. Kobzar · O. Shekera · V. Shevchenko

Institute of Macromolecular Chemistry, National Academy of Sciences of Ukraine, Kharkivske Shosse 48, Kyiv 02160, Ukraine

e-mail: ttkachenkoim@gmail.com

[15]. It has been recognized that azo-azomethine organic chromophores combine the valuable properties of both imine and azo groups. The simultaneous combination of such groups within the molecule conjugation system leads to the bathochromic shift of the absorption bands in the electronic spectra, increases stability of the *cis*-isomer of the azo group and photostability, and at the same time provides the low oxidation state of metal ions [25–27]. Thus, there are many motivations to explore new azo-azomethine conjugated systems and it is not surprising, therefore, that currently, a specific attention is drawn to the polymer-based materials [25, 27–29] as well as organic azo-azomethine chromophores [26, 30–33] having both azo and azomethine groups.

Previously, we developed two polyazomethines with azo groups in the backbone (Azo-Pam) by polycondensation of tetrafluorobenzene- or octafluorobiphenylene-based bis-hydroxybenzaldehydes with hexamethylenediamine [29, 34]. Both polymers showed promising potential as light-sensitive polymers for creation of polarization holograms and various liquid crystal device fabrications. Additionally, the obtained data show that used monomers, namely *meta*-linked azo-containing bis(2-hydroxybenzaldehyde)s with perfluorinated aromatic fragments, are effective building blocks for designing a wide range of stimuli-responsive and optical active materials. These monomers contain *ortho*-oriented hydroxy groups to aldehyde functions, and hence, the optical properties and the switching dynamics of azobenzenes can be controlled through *ortho*-substitution [35–37]. Next, it was determined that presence of fluorinated electron-withdrawing units in monomers and corresponding polymers resulted in their good optical properties, thermostability, and improved solubility [29, 38]. Though, an increased content of aliphatic units in the mentioned Azo-Pam polymers led to some natural deterioration of their thermal stability and shortening of the π -conjugation chain length. Extending the π -conjugated systems of chromophore-based compounds is the most promising strategy to design efficient visible-light-driven switches due to a more obvious red-shift of π - π^* transition electronic bands [14, 16, 39]. In this context, it was anticipated that replacing of aliphatic diamine with aromatic one would improve functional properties of resulting Azo-Pam.

Insufficient solubility appeared to be a major drawback for fully aromatic polymers, especially for main-chain polyazobenzenes and polyazomethines [25, 40, 41]. It is generally recognized that the presence of flexible ether linkages and isomeric fragments in a polymer backbone allows regulating the different properties (optical and liquid crystalline properties, thermostability) of the final materials as well as enhances their solubility [29, 41]. Additionally, one of the successful approaches for enhancement of solubility is the decreasing of molecular weight of the targeted polymers, viz., the development of oligomers. To date, several types of azobenzene- [42, 43] or imine-based oligomers [14, 44, 45] have been reported.

Herein, we report on the synthesis of novel aldehyde-terminated azo-containing oligoazomethine with both tetrafluorobenzene and octafluorobiphenylene units as well as ether linkages and *meta*-oxyphenylene fragments in the backbone. Properties of the synthesized oligomer, such as solubility, tensile strength, thermal stability, photooptical behavior, and photoinductive birefringence, were investigated.

23.2 Experimental Section

23.2.1 Materials

Monomers 3,3'-((2,3,5,6-tetrafluoro-1,4-phenylene)bis[oxy-3,1-phenylenediazene-2,1-diyl])bis(6-hydroxybenzaldehyde) **1** and 3-([4'-(3-aminophenoxy)-2,2',3,3',5,5',6,6'-octafluoro-1,1'-biphenyl-4-yl]oxy)phenyl amine **2** were prepared as described earlier [38, 46]. 2-aminophenol (Acros Organics, 99%) was used as received. The other reagents and solvents were purified routinely.

23.2.2 Synthesis of Azo-Oam-1

A dry, 25 ml three-necked flask equipped with an oil bath, a mechanical stirrer, a cold water condenser, an argon inlet/outlet, and a thermometer was charged with monomer **1** (0.300 g, 0.476 mmol), diamine **2** (0.213 g, 0.416 mmol), and 3 ml of N,N-dimethylacetamide (DMAc). The mixture was then heated to 110 °C and stirred vigorously at this temperature for 24 h. The reaction mixture was quenched with methanol, and the resulting solid was collected by filtration. The oligomer was purified by reprecipitation from DMAc solution into methanol and then dried in a vacuum oven at 60 °C overnight—yield 86%; FTIR (KBr, cm⁻¹): 3600–3300 (–OH), 3100–2850 (C–H), 1668 (–CHO, end-group stretching), 1625 (–CH = N–), 1597, 1485 (C = C, arom.), 1221 (C–O–C), and 995, 980 (C–F); and UV–Vis spectrum (DMAc, 15.0 μg/mL): λ_{max1} = 364 nm and λ_{max2} = 464 nm.

23.2.3 Synthesis of Model Compound 3 (4,4'-((((perfluoro-1,4-phenylene)bis(oxy))bis(3,1-phenylene))bis(diazene-2,1-diyl))bis(2-(((2-hydroxyphenyl)imino)methyl)phenol))

Compound **1** (0.500 g, 0.793 mmol), 2-aminophenol (0.173 g, 1.586 mmol), and DMAc (4.0 ml) were mixed and stirred until the solids were dissolved. Then, the solution was heated at 80 °C for 4 h. After cooling, the reaction mixture was precipitated into methanol. The resulting solid was collected by filtration, washed with hot methanol for three times, and finally dried at 60 °C under vacuum—yield 78% ¹H NMR (DMSO-*d*₆, 400 MHz, ppm): δ 15.07 (s, 2H, OH), 10.10 (s, 2H, OH), 9.20 (s, 2H, CH = N), 8.24 (s, 2H, Ph), 7.99 (d, 2H, *J* = 7.5 Hz, Ph), 7.68–7.64 (m, 6H, Ph), 7.52 (d, 2H, *J* = 5.6 Hz, Ph), 7.41 (s, 2H, Ph), 7.02 (br.s., 4H, Ph), and 6.93 (d, 2H, *J* = 5.6 Hz, Ph); ¹⁹F NMR (DMSO-*d*, 376 MHz, ppm): δ –154.85 (s, 4F, Ph), %; FTIR (KBr, cm⁻¹): 3600–3000 (–OH), 3050–2850 (C–H), 1618 (–CH = N–)– 1589,

1499 (C=C, arom.), 1246 (C–O–C), and 1016, 993 (C–F); and UV–Vis spectrum (DMAc, 6.0 $\mu\text{g/mL}$): $\lambda_{1\text{max}} = 368 \text{ nm}$ and $\lambda_{2\text{max}} = 459 \text{ nm}$.

23.2.4 Characterization

Fourier transform infrared (FTIR) spectra ($4000\text{--}400 \text{ cm}^{-1}$) of the synthesized compounds were recorded on a TENSOR 37 spectrometer in KBr pellets. ^1H and ^{19}F NMR spectra were recorded on a Bruker Avance instrument at room temperature in DMSO-*d*₆. Chemical shifts for ^1H NMR are given relative to dimethyl sulfoxide ($\delta = 2.50 \text{ ppm}$). For ^{19}F NMR, chemical shifts are reported in the scale relative to CFCl_3 . The UV–Vis spectra of the obtained compounds were recorded on a Shimadzu UV-2450 spectrophotometer. The Azo-Oam-1 film for mechanical analysis was prepared by casting from DMAc solution (0.25 mg/mL) onto the Teflon plate. The obtained film was dried at room temperature for 24 h and then dried under vacuum for 24 h at 40 °C. Tensile strength (TS) was measured on a 2166 P-5 tensile-testing machine with uniaxial tension at a rate of clamp movement of 50 mm/min. The DSC analysis was run using a TA Q200 instrument; heating rate was 20 °C/min under an air atmosphere. The thermo-oxidative destruction of polymers was studied using the thermal gravimetric analysis (TGA) with a TA Instruments Q-50 apparatus (USA) in air. A heating rate of 20 °C/min with a temperature from 20 to 700 °C was applied.

The investigation of the pH influence upon the UV–Vis absorption maxima in DMAc was conducted at an oligomer concentration of 0.006 mg/mL by adding 1 drop of 1 N HCl solution to the corresponding oligomer solution in order to form an acid medium and by adding 2 drops of 1 N NaOH solution to the acid solution of oligomer in order to achieve acid neutralization and to form alkaline medium. Photoisomerization experiment in solution was performed by irradiating the samples at 10 cm distance with 365 nm UV light from DeLux EBT-01 mercury lamp (26 W) and then recorded. For the solid-state photoisomerization, the Azo-Oam-1 oligomer film was irradiated by UV light ($\lambda = 370 \text{ nm}$, 3.4 mW/cm^2) at 4 cm distance.

The measurements of photoinduced birefringence in the Azo-Oam-1 oligomer film (film thickness $\sim 80 \mu\text{m}$) were carried out with an experimental optical setup as described in [29, 47]. Briefly, the Azo-Oam-1 film was irradiated with polarized light of an Ar laser ($\lambda = 532 \text{ nm}$, 50 mW/cm^2) and was simultaneously located between the crossed polarizers for a He–Ne laser ($\lambda = 628 \text{ nm}$, 5 mW) as a probe beam. The polarization direction of the irradiating light made up a 45° to the directions of the polarizer and analyzer. The change in birefringence of the sample during the irradiation was monitored as a function of illumination time. In the Azo-Oam-1 film, the gratings were formed by two spatially modulated Ar laser with $P = 10 \text{ mW/cm}^2$ at 532 nm with two linear p-polarizations. The recording of the polarized gratings was performed using experimental scheme represented in [48].

23.3 Results and Discussion

23.3.1 Synthesis and General Properties of Azo-Oam-1 Oligomer

The desired new fluorinated 2-hydroxybenzaldehyde-terminated oligomer (Azo-Oam-1) was prepared in good yield by the interaction of *meta*-linked diamine **2** with excess of azo-containing tetrafluorobenzene-based dialdehyde **1** in DMAc with following the general reaction pathway depicted in Fig. 23.1a. The oligomer repeating unit was targeted as $n = 7$ by controlling the molar ratio of dialdehyde **1** to diamine **2**. Note that we originally sought out to synthesize azo-based polyazomethine from equivalent molar amounts of monomers **1** and **2**, but the obtained polymer product was insoluble in any of the tested solvents. This phenomenon is ascribed by the high molecular weight of the rigid aromatic polymer chains, which limits the mobility of these chains.

The synthesized oligomer was obtained as yellow fibrous solid, soluble in DMAc and *N*-methyl-2-pyrrolidone, only partially soluble in *N,N*-dimethylformamide, and insoluble in the other organic solvents, such as DMSO, THF, acetone, and chloroform. The chemical structure of Azo-Oam-1 was studied by FTIR spectroscopy (Fig. 23.1b, spectrum 2); the FTIR spectrum of the initial monomer **1** is shown for comparison (Fig. 23.1b, spectrum 1). Thus, the appearance of the absorption band at 1625 cm^{-1}

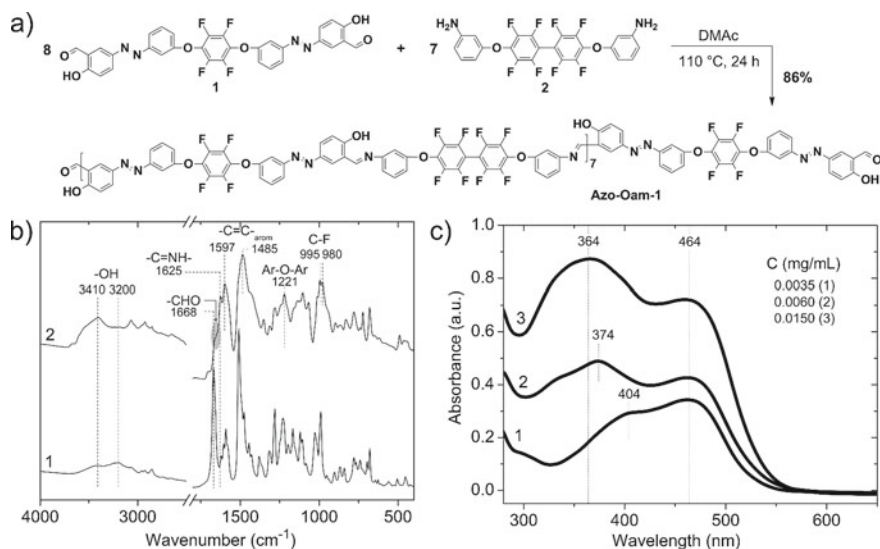


Fig. 23.1 a Synthesis of Azo-Oam-1 oligomer. b FTIR spectra of the initial monomer **1** (spectrum 1) and synthesized Azo-Oam-1 oligomer (spectrum 2). c UV-Vis absorbance spectra of Azo-Oam-1 at various concentrations ($3.5, 6.0$ and $15.0\ \mu\text{g mL}^{-1}$) in DMAc

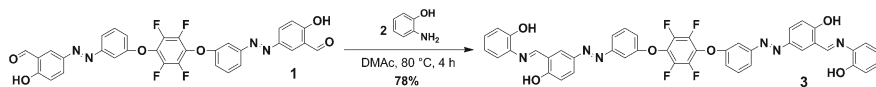


Fig. 23.2 Scheme of model compound **3** synthesis

indicates formation of $-\text{CH}=\text{N}-$ linkages in oligomer. The strong absorption band at 1668 cm^{-1} in the spectrum of monomer **1** was assigned to the aldehyde groups, and because of polymerization process, this band almost completely disappeared in the spectrum of Azo-Oam-1. Meanwhile, the weak peak (as a shoulder) around 1660 cm^{-1} in the spectrum of Azo-Oam-1 indicates the presence of aldehyde end groups. The Ar-OH bands are located at about the range $3200\text{--}3600\text{ cm}^{-1}$ in azo-azomethine-based oligomer. Additionally, the FTIR spectrum of the target oligomer shows peaks which correspond to $\text{C}-\text{F}$ (980 and 995 cm^{-1}), $\text{Ar}-\text{O}-\text{Ar}$ (1221 cm^{-1}), $\text{C}=\text{C}_{\text{arom}}$ (1485 and 1597 cm^{-1}), and CH groups ($2850\text{--}3100\text{ cm}^{-1}$) (Fig. 23.1b).

^1H NMR analysis of the low molar mass material (a mixture of dimers and trimers) removed from the initial stage of polymer synthesis confirms the azomethine bond formation by the appearance of the characteristic imine peak in the range of $9.2\text{--}9.4$ ppm. Note that two azomethine peaks were detected because the mixture of dimers and trimers possesses nonequivalent imines. Additionally, the formation of the azomethine linkage between dialdehyde **1** and aromatic amine was proved by the NMR, FTIR, and UV-Vis techniques on the base of the newly synthesized azo-azomethine model compound **3** (Fig. 23.2). The main characteristic peaks in the above-mentioned spectra for the Azo-Oam-1 coincide with similar peaks in the model compound **3**. Thus, for instance, the peak at 1618 cm^{-1} (FTIR) shows the presence of azomethine bond, as in the final oligomer.

Spectral features of the $-\text{CH}=\text{N}-$ and $-\text{N}=\text{N}-$ groups are closed, where their transitions are overlapped [33]. As it is depicted in Fig. 23.1c, the UV-Vis spectrum of Azo-Oam-1 are characterized by two absorption band, but position and relative intensity of these bands depend on the concentration of the oligomer in the DMAc. An absorption band related to the $\pi \rightarrow \pi^*$ transitions appears at $364\text{--}404\text{ nm}$, while an abroad intense band in the visible region at 464 nm characterizes the $n \rightarrow \pi^*$ transitions, intramolecular charge transfer interaction involving the conjugated azo-azomethine blocks and hydrogen-bonded complexes of the obtained oligomers with the highly polar aprotic solvent such as DMAc [29, 46]. Generally, the reducing of the concentration of oligomer in a solution has caused a bathochromic shift of the $\pi \rightarrow \pi^*$ absorption band and increasing relative intensity of the $n \rightarrow \pi^*$ transition.

Importantly, despite the oligomeric nature, Azo-Oam-1 forms flexible free-standing film (the TS value of ca. 13 MPa) by casting from DMAc solution. From this point of view, the resulting oligomer can be considered as a polymer system. Notably, in general, the majority of azo-azomethine-containing polymers as well as aromatic main-chain polyazobenzenes and polyazomethines described in the literature have often a fairly low molecular weight [19, 25, 41].

The thermal properties of Azo-Oam-1 film were investigated using DSC and TGA techniques (Fig. 23.3).

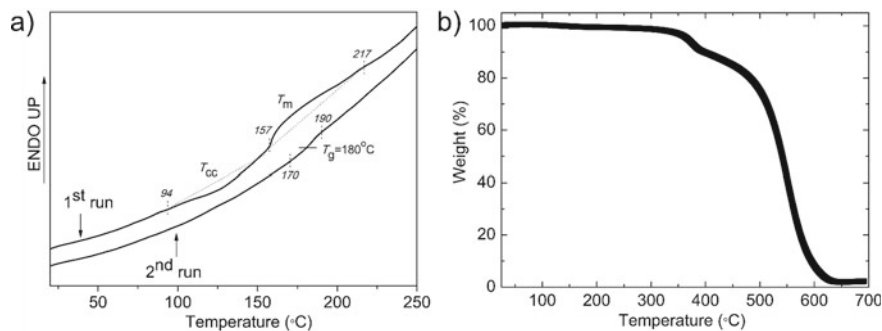


Fig. 23.3 **a** DSC curves of Azo-Oam-1 oligomer recorded for film samples; depicted are the first and second heating runs (DSC curves are offset for clarity). Air atmosphere, heating rate of 20 °C/min. **b** TGA curve of Azo-Oam-1 in an air atmosphere (heating rate: 20 °C/min with a temperature from 25 to 700 °C)

Oligomer sample exhibited a broad exothermic peak at the temperature range of 94–157 °C followed by a broad endothermic peak from 157 to 217 °C in DSC analysis, during the first heating run (Fig. 23.3a). The first exothermic peak indicates formation of some ordered structures due to a cold crystallization process (T_{cc}), and the second peak (T_m) is related to the melting of such formed ordered phase. Generally, multiple phase transitions on the DSC profiles are characteristic of chromophore-containing polymers, especially polyazomethines [41, 49]. Nevertheless, during the second heating the oligomer showed only a glass transition (T_g) at 180 °C, which basically indicates the amorphous nature of this sample (Fig. 23.3a). The glass transition region value of the oligomer is 20 °C. The obtained oligomer is thermally stable in air up to 350 °C (Fig. 23.3b), showing only a 3% weight loss at this temperature. The replacement of the aliphatic diamine (namely 1,6-hexamethylenediamine) by an aromatic one (diamine **2**) induces an important increase in the thermostability of Azo-Oam-1. Thus, the results of TGA for Azo-Oam-1 obviously indicate the 5% weight-loss temperature ($T_{5\%}$) at 365 °C, which is higher than that of the azo-containing polyazomethine prepared from monomer **1** and aliphatic 1,6-hexamethylenediamine ($T_{5\%}$ is about 300 °C) [29, 34].

23.3.2 Optical Properties of Oligomer

As discussed above, it was found that changing the concentration of oligomer in solvent played a significant role in regulating its absorption maxima (Fig. 23.1c). Additionally, in DMAc solution, the absorption maxima of Azo-Oam-1 oligomer can be intentionally regulated by changing the pH values of a medium. For example, a hypsochromic shift from ~ 374 to 344 nm is clearly observed when increasing the proton concentration in the solution (pH ~2) while the peak at 464 nm disappears (Fig. 23.4a). When the neutralization of phenol groups of the oligomer in the alkaline

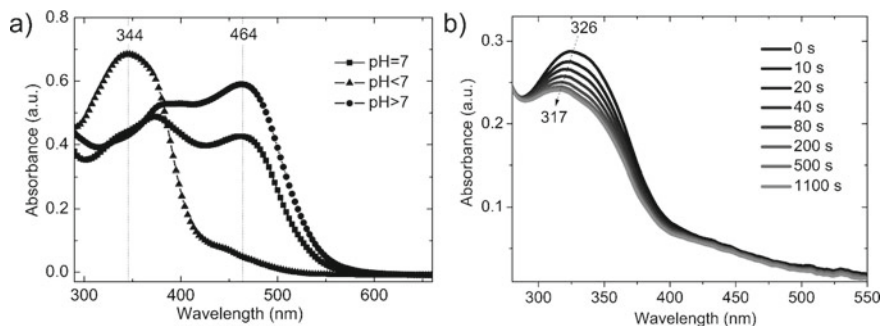


Fig. 23.4 **a** UV-Vis spectra of Azo-Oam-1 in DMAc at acidic ($\text{pH} < 7$), neutral ($\text{pH} = 7$), and alkaline medium ($\text{pH} > 7$). **b** Photoisomerization of Azo-Oam-1 in DMAc (0.006 mg/mL) upon irradiation at 365 nm

medium was performed ($\text{pH} \sim 12$), the absorption spectrum changes significantly: The absorptivity in the visible wavelengths (the $n-\pi^*$ band at 464 nm) increases multifold in comparison to spectrum of protonated Azo-Oam-1 (Fig. 23.4a). Such distribution of the absorption maxima (the difference makes up 120 nm) is a consequence of the formation of ionic form in alkaline medium and azo form in acidic medium [29, 46].

The ability of azobenzene-based compounds to undergo photoisomerization is an effective tool for regulating their properties. The *trans-cis* transition of Azo-Oam-1 in the DMAc solution was not registered. At the same time, the reversible *trans-cis-trans* photoisomerization in the Azo-Oam-1 film is observed under UV illumination for *trans-cis* isomerization (Fig. 23.4b) and under deuterium lamp irradiation for the reversible *cis-trans* relaxation of azobenzene units.

23.3.3 Light-Induced Birefringence and Diffraction Gratings in the Azo-Oam-1 Film

One of the greatest opportunities for light-sensitive polymers comes from their ability to become anisotropic under a polarized light irradiation. Photoinduced anisotropy in the synthesized Azo-Oam-1 oligomer was investigated through birefringence and diffraction grating recording process. It is shown that after the beginning of irradiation with polarized light, the intensity of birefringence in the Azo-Oam-1 film increases and at a certain time reaches a constant value (Fig. 23.5a). After switching off the irradiation light, the relaxation process (between B and C time points, Fig. 23.5a) can be observed for oligomer sample due to *cis-trans* isomerization of azo groups. The obtained results are typical for the photoisomerization behavior in polymers accompanied by the motions of the azobenzene chromophores and the interactions of orientated azobenzene groups [25, 50, 51]. It is important to note that when the writing beam is turned off (point B, Fig. 23.5a), the remaining anisotropy continues to

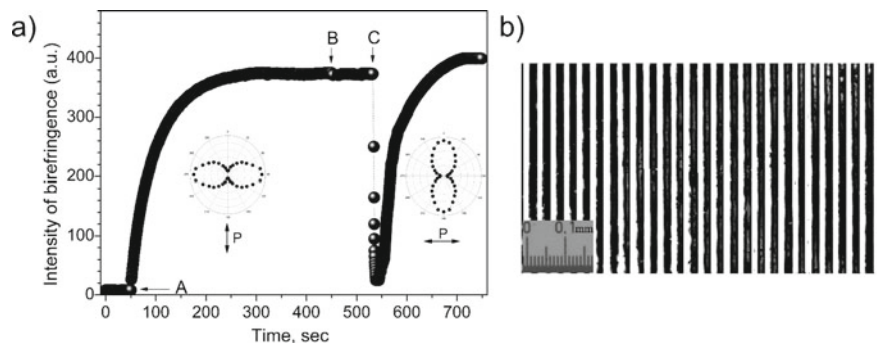


Fig. 23.5 **a** Dependence intensity of birefringence in Azo-Oam-1 film on irradiation time from Ar laser ($\lambda = 532$ nm, $P = 10$ mW). Linearly polarized light is switched on at point A (vertical polarization) and switched off at point B; irradiation when rotating the polarization of light by 90° (horizontal polarization) is switched on at point C. The insets show absorption spectra of Azo-Oam-1 for vertical (left inset) and horizontal (right inset) polarization of the incident polarized light. **b** Optical image of the diffraction pattern in Azo-Oam-1 film in a polarize microscope (scale = 0.1 mm)

hold at a certain value and this remnant birefringence is very stable for the oligomeric film. We assume that the main reason of the high residual anisotropy is the significant intermolecular interaction of macromolecules, which partially fix (stabilize) the *cis*-stationary state of azobenzene fragments in the Azo-Oam-1 film. Potentially, such interactions are possible with the groups $-\text{OH}$ and $-\text{CH}=\text{N}-$, which are capable of forming a stable hydrogen-bond network as well as between non-fluorinated and fluorinated aromatic fragments ($\pi_{\text{Ar}} - \pi_{\text{ArF}}$ stacking interactions) [23, 29].

While we observed the relaxation in the oligomer film, the direction of the irradiating polarization of Ar laser, due to the rotation of the Glan–Thompson prism, was changed by 90° and the irradiating beam was turned on again. Figure 23.5a shows that initially the intensity of birefringence decreases, apparently due to reduction or “erasure” of the anisotropy (Δn changes), and then increases rapidly, again reaching a steady state, which indicates an increase in anisotropy in the film according to new direction of polarization of the irradiating beam. Thus, so-called the phenomenon of “rewriting” was observed, which indicates a change in the birefringence in accordance with the change in the direction of irradiating polarization. Direction of the photoinduced anisotropy in the Azo-Oam-1 film is perpendicular to the direction of irradiation polarization light ($\lambda = 532$ nm). It was confirmed by the angular dependence of the polarized light absorption (Fig. 23.5a, insets).

Azo-Oam-1 oligomer was used for recording of diffraction gratings. Gratings were formed by 2-beam irradiation of Azo-Oam-1 film by spatially modulated Ar laser (wavelength $\lambda = 532$ nm, power $P \leq 10$ mW) with two linear *p*-polarizations. The optical scheme for recording diffraction gratings was described in [48]. The observed diffraction patterns demonstrate equal intensities in each diffraction order (+1; –1) which is monitored as a function of recording time. The photo of the recorded diffraction grating with a resolution ~ 30 lines per millimeter made with polarized

microscope is represented in Fig. 23.5b. Having the probe beam intensities of the zero-diffraction order, I_0 , and $I_{\pm 1}$ diffraction order, we can determine ($\eta_{\pm 1} = \frac{I_{\pm 1}}{I_0} * 100\%$) the efficiency of diffraction as $\sim 2\%$. This efficiency of diffraction gratings looks promising for further applications.

23.4 Conclusion

In a summary, we have developed synthetic route for a novel *meta*-linked aromatic oligomer with the aldehyde end groups and possessing both azo and azomethine groups as well as mono- and biphenylene perfluorinated aromatic units. The obtained oligomer has excellent solubility in common organic solvents and exhibited good thermal properties. The benefits of the proposed oligomer structure are its ability to form thermostable ($T_{5\%} = 365\text{ }^\circ\text{C}$) mechanically stable (TS = 13 MPa) free-standing film in which *trans*–*cis* photoisomerization occurs. The presence of OH groups at the *ortho* position with respect to the imine linkage in the azo-based oligoazomethine contributes to the reversible intramolecular migration of the proton of the hydroxyl groups, which allows to regulate their absorption maximum within the wide range by changing the concentration of oligomer and pH of the DMAc solution. It was found that after the irradiation by the polarized light the resulting oligomer acquired time stable anisotropic properties. Moreover, holographic gratings (efficiency of diffraction about 2%.) were observed in the oligomer film irradiated with two polarized beams. Doubtlessly, there are still many challenging options to be studied, but the obtained preliminary data show that the synthesis strategy of the azo-azomethine oligomer is an effective instrument for designing a wide range of stimuli-responsive and optical active materials.

Acknowledgements This work was performed within the target complex program of basic research of the National Academy of Sciences of Ukraine within the projects B/197 “Liquid crystal colloids: properties and applications”, №16(6541230) “Hierarchy of structures in complex liquid crystal systems. Physical properties and applications”, and National Research Foundation of Ukraine 2020.01/0144 “Flexible Printable Humidity Sensing Elements on Lyotropic Chromonic Liquid Crystals”. The work was partially supported by Ukraine Scholars Fund at AMLCI&KSU. The authors are grateful of Dr. S. Kredentser for help in photography of the diffraction pattern in Azo-Oam-1 film in a polarize microscope.

Conflicts of Interest

On behalf of all authors, the corresponding author states that there is no conflict of interest.

References

1. Liu F, Urban MW (2010) Recent advances and challenges in designing stimuli-responsive polymers. *Prog Polym Sci* 35:3–23. <https://doi.org/10.1016/j.progpolymsci.2009.10.002>
2. Cao ZQ, Wang GJ (2016) Multi-stimuli responsive polymer materials: particles, films, and bulk gels. *Chem Rec* 16:1398–1435. <https://doi.org/10.1002/tcr.201500281>
3. Ohtani S, Yamada N, Gon M, Tanaka K, Chujo Y (2021) The effect of alkyl chain lengths on the red-to-near-infrared emission of boron-fused azomethine conjugated polymers and their film-state stimuli-responsivities. *Polym Chem* 12:2752–2759. <https://doi.org/10.1039/D1PY00213A>
4. Pang X, Lv JA, Zhu C, Qin L, Yu Y (2019) Photodeformable azobenzene-containing liquid crystal polymers and soft actuators. *Adv Mater* 31:1904224. <https://doi.org/10.1002/adma.201904224>
5. Stuart M, Huck W, Genzer J, Müller M, Ober C, Stamm M, Sukhorukov G, Szleifer I, Tsukruk V, Urban M, Winnik F, Zauscher S, Luzinov I, Minko S (2010) Emerging applications of stimuli-responsive polymer materials. *Nature Mater* 9:101–113. <https://doi.org/10.1038/nmat2614>
6. Moulin E, Faour L, Carmona-Vargas CC, Giuseppone N (2020) From molecular machines to stimuli-responsive materials. *Adv Mater* 32:1906036. <https://doi.org/10.1002/adma.201906036>
7. Kuenstler AS, Clark KD, Read de Alaniz J, Hayward RC (2020) Reversible actuation via photoisomerization-induced melting of a semicrystalline poly(azobenzene). *ACS Macro Lett* 9:902–909. <https://doi.org/10.1021/acsmacrolett.0c00328>
8. Wang HZ, Chow HF (2018) A photo-responsive poly(amide-triazole) physical organogel bearing azobenzene residues in the main chain. *Chem Commun* 54:8391–8394. <https://doi.org/10.1039/C8CC05096A>
9. Wu S, Butt HJ (2020) Solar-thermal energy conversion and storage using photoresponsive azobenzene-containing polymers. *Macromol Rapid Commun* 41:1900413. <https://doi.org/10.1002/marc.201900413>
10. Gon M, Tanaka K, Chujo Y (2021) Discovery of functional luminescence properties based on flexible and bendable boron-fused azomethine/azobenzene complexes with O, N, O-type tridentate ligands. *Chem Rec* 21:1358–1373. <https://doi.org/10.1002/tcr.202000156>
11. Lim W, Oo C, Choo Y, Looi S (2015) New generation of photosensitive poly(azomethine)esters: thermal behaviours, photocrosslinking and photoluminescence studies. *Polymer* 71:15–22. <https://doi.org/10.1016/j.polymer.2015.06.041>
12. Çulhaoğlu S, Kolcu F, Kaya İ (2021) Synthesis of phosphate and silane-based conjugated polymers derived from bis-azomethine: Photophysical and thermal characterization. *React Funct Polym* 166:104978. <https://doi.org/10.1016/j.reactfunctpolym.2021.104978>
13. Li G, Yu K, Noordijk J, Meeusen-Wierds M, Gebben B, oude Lohuis P, Schotman A, Bernaerts K (2020) Hydrothermal polymerization towards fully biobased polyazomethines. *Chem Commun* 56:9194–9197. <https://doi.org/10.1039/D0CC03026K>
14. Liu M, Yin L, Wang L, Miao T, Cheng X, Wang Y, Zhang W, Zhu X (2019) Synthesis of monodisperse aromatic azo oligomers toward gaining new insight into the isomerization of π -conjugated azo systems. *Polym Chem* 10:1806–1811. <https://doi.org/10.1039/C9PY00001A>
15. Gon M, Tanaka K, Chujo Y (2018) A highly efficient near-infrared emissive copolymer with a N=N double-bond π -conjugated system based on a fused azobenzene-boron complex. *Angew Chem* 130:6656–6661. <https://doi.org/10.1002/ange.201803013>
16. Anwar N, Willms T, Grimme B, Kuehne AJ (2013) Light-switchable and monodisperse conjugated polymer particles. *ACS Macro Lett* 2:766–769. <https://doi.org/10.1021/mz400362g>
17. Tkachenko IM, Ledin PA, Shevchenko VV, Tsukruk VV (2021) Mixed star-shaped POSS-based molecule with hydroxy group-containing units and azobenzene fragments as two types of arms. *Mendeleev Commun* 31:27–29. <https://doi.org/10.1016/j.mencom.2021.01.007>

18. Kang H, Joo K, Kang Y, Lee J, Lee Y, Jeon I, Lee T, Koh W, Choi J, Kim H, Ka J (2021) Highly sensitive updatable green hologram recording polymer with photoisomerizable azobenzene with highly birefringent acetylene as the side chain. *Polym J* 53:539–547. <https://doi.org/10.1038/s41428-020-00447-x>
19. Nitschke P, Jarzabek B, Damaceanu MD, Bejan AE, Chaber P (2021) Spectroscopic and electrochemical properties of thiophene-phenylene based Schiff-bases with alkoxy side groups, towards photovoltaic applications. *Spectrochim Acta A Mol Biomol Spectrosc* 248:119242. <https://doi.org/10.1016/j.saa.2020.119242>
20. Khalid N, Iqbal A, Siddiqi HM, Park OO (2017) Synthesis and photophysical study of new green fluorescent TPA based poly(azomethine)s. *J Fluoresc* 27:2177–2186. <https://doi.org/10.1007/s10895-017-2157-4>
21. Kato T, Gon M, Tanaka K, Chujo Y (2021) Modulation of stimuli-responsiveness toward acid vapor between real-time and write-erase responses based on conjugated polymers containing azobenzene and Schiff base moieties. *J Polym Sci* 59:1596–1602. <https://doi.org/10.1002/pol.20210329>
22. Ghoneim M, El-Sonbati A, Diab M, El-Bindary A, Serag L (2015) Supramolecular assembly on coordination of azopolymer complexes: a review. *Polymer Plast Tech Eng* 54:100–117. <https://doi.org/10.1080/03602559.2014.935399>
23. Iwan A, Sek D (2008) Processible polyazomethines and polyketanils: from aerospace to light-emitting diodes and other advanced applications. *Prog Polym Sci* 33:289–345. <https://doi.org/10.1016/j.progpolymsci.2007.09.005>
24. Sobarzo PA, Terraza CA, Maya EM (2020) New efficient tetraphenyl silylated poly (azomethine)s based on “pincer-like” bis(imino) pyridine iron (III) complexes as heterogeneous catalysts for CO₂ conversion. *Eur Polym J* 126:109567. <https://doi.org/10.1016/j.eurpolymj.2020.109567>
25. Kovalchuk AI, YaL K, Tkachenko IM, Shevchenko VV (2019) Polymers containing azo and azomethine groups: synthesis, properties, and application. *Polym Sci Ser B* 61:109–123. <https://doi.org/10.1134/S1560090419020040>
26. Georgiev A, Kostadinov A, Ivanov D, Dimov D, Stoyanov S, Nedelchev L, Nazarova D, Yancheva D (2018) Synthesis, spectroscopic and TD-DFT quantum mechanical study of azo-azomethine dyes, a laser induced *trans-cis-trans* photoisomerization cycle. *Spectrochim Acta A Mol Biomol Spectrosc* 192:263–274. <https://doi.org/10.1016/j.saa.2017.11.016>
27. Hajibeygi M, Shafiei-Navid S, Shabani M, Vahabi H (2018) Novel poly(amide-azomethine) nanocomposites reinforced with polyacrylic acid-co-2-acrylamido-2-methylpropanesulfonic acid modified LDH: Synthesis and properties. *Appl Clay Sci* 157:165–176. <https://doi.org/10.1016/j.clay.2018.03.004>
28. Diana R, Panunzi B, Shikler R, Nabha S, Caruso U (2019) A symmetrical azo-based fluorophore and the derived salen multipurpose framework for emissive layers. *Inorg Chem Commun* 104:186–189. <https://doi.org/10.1016/j.inoche.2019.04.016>
29. Kovalchuk A, Kobzar Ya, Tkachenko I, Kurioz Yu, Tereshchenko O, Shekera O, Nazarenko V, Shevchenko V (2019) Photoactive fluorinated poly(azomethine)s with azo groups in the main chain for optical storage applications and controlling liquid crystal orientation. *ACS Appl Polym Mater* 2:455–463. <https://pubs.acs.org/doi/https://doi.org/10.1021/acsapm.9b00906>
30. Ozkan G, Kose M, Zengin H, McKee V, Kurtoglu M (2015) A new Salen-type azo-azomethine ligand and its Ni(II), Cu(II) and Zn(II) complexes: synthesis, spectral characterization, crystal structure and photoluminescence studies. *Spectrochim Acta A Mol Biomol Spectrosc* 150:966–973. <https://doi.org/10.1016/j.saa.2015.06.038>
31. Khanmohammadi H, Darvishpour M (2009) New azo ligands containing azomethine groups in the pyridazine-based chain: synthesis and characterization. *Dyes Pigm* 81:167–173. <https://doi.org/10.1016/j.dyepig.2008.07.019>
32. Iftime M, Cozan V, Airinei A, Varganici C, Ailiesei G, Timpu D, Sava I (2019) Asymmetric azomethine amines with azobenzene moieties-liquid crystalline and optical properties. *Liq Cryst* 46:1584–1594. <https://doi.org/10.1080/02678292.2019.1640903>

33. Stoilova A, Georgiev A, Nedelchev L, Nazarova D, Dimov D (2019) Structure-property relationship and photoinduced birefringence of the azo and azo-azomethine dyes thin films in PMMA matrix. *Opt Mater* 87:16–23. <https://doi.org/10.1016/j.optmat.2018.07.010>
34. Tkachenko I, Kurioz Y, Kovalchuk A, Ya K, Shekera O, Tereshchenko O, Nazarenko V, Shevchenko V (2020) Optical properties of azo-based poly(azomethine)s with aromatic fluorinated fragments, ether linkages and aliphatic units in the backbone. *Mol Cryst Liq Cryst* 697:85–96. <https://doi.org/10.1080/15421406.2020.1731080>
35. Dong M, Babalhavaeji A, Samanta S, Beharry A, Woolley G (2015) Red-shifting azobenzene photoswitches for in vivo use. *Acc Chem Res* 48:2662–2670. <https://doi.org/10.1021/acs.accounts.5b00270>
36. Ahmed Z, Siiskonen A, Virkki M, Priimagi A (2017) Controlling azobenzene photoswitching through combined ortho-fluorination and -amination. *Chem Commun* 53:12520–12523. <https://doi.org/10.1039/C7CC07308A>
37. Han M, Honda T, Ishikawa D, Ito E, Hara M, Norikane Y (2011) Realization of highly photoreponsive azobenzene-functionalized monolayers. *J Mater Chem* 21:4696–4702. <https://doi.org/10.1039/C0JM03697H>
38. Kovalchuk AI, YaL K, Tkachenko IM, Tolstov AL, Shekera OV, Shevchenko VV (2017) Synthesis and optical properties of new isomeric azo-containing bis(2-hydroxybenzaldehydes) with tetrafluorobenzene units. *Mendeleev Commun* 27:599–601. <https://doi.org/10.1016/j.mencom.2017.11.020>
39. Wang K, Yin L, Miu T, Liu M, Zhao Y, Chen Y, Zhou N, Zhang W, Zhu X (2018) Design and synthesis of a novel azobenzene-containing polymer both in the main- and side-chain toward unique photocontrolled isomerization properties. *Mater Chem Front* 2:1112–1118. <https://doi.org/10.1039/C8QM00035B>
40. Younis M, Long J, Peng S-Q, Wang X-S, Chai C, Bogliotti N, Huang M-H (2021) Reversible transformation between azo and azonium bond other than photoisomerization of azo bond in main-chain polyazobenzenes. *J Phys Chem Lett* 12:3655–3661. <https://doi.org/10.1021/acs.jpcclett.1c00750>
41. YaL K, Tkachenko IM, Bliznyuk VN, Shekera OV, Turiv TM, Soroka PV, Nazarenko VG, Shevchenko VV (2016) Synthesis and characterization of fluorinated poly(azomethine ether)s from new core-fluorinated azomethine-containing monomers. *Des Monomers Polym* 19:1–11. <https://doi.org/10.1080/15685551.2015.1092007>
42. King ED, Tao P, Sanan TT, Hadad CM, Parquette JR (2008) Photomodulated chiral induction in helical azobenzene oligomers. *Org Lett* 10:1671–1674. <https://doi.org/10.1021/ol8004722>
43. Liu M, Shi X, Li L, Zhang J, Huang Z, Zhang W, Zhou N, Zhang Z, Zhu X (2021) Synthesis of discrete conjugated fluorine azo oligomers for the investigation of azobenzene position dependent physical properties and photoreponsive behavior. *Macromol Chem Phys* 222:2100092. <https://doi.org/10.1002/macp.202100092>
44. Özyaytekin İ, Kar Y (2012) Synthesis and properties of composites of oligoazomethine with char. *J Appl Polym Sci* 123:815–823. <https://doi.org/10.1002/app.34509>
45. Tundidor-Camba A, González-Henríquez CM, Sarabia-Vallejos MA, Tagle LH, Hauyón RA, Sobarzo PA, González A, Ortiz PA, Maya EM, Terraza CA (2018) Silylated oligomeric poly(ether-azomethine)s from monomers containing biphenyl moieties: synthesis and characterization. *RSC Adv* 8:1296–1312. <https://doi.org/10.1039/C7RA10929F>
46. Kovalchuk AI, YaL K, Tkachenko IM, Tolstov AL, Shekera OV, Shevchenko VV (2018) Synthesis and optical properties of new isomeric core-fluorinated azo-containing bis(2-hydroxybenzaldehyde)s. *J Mol Struct* 1173:671–678. <https://doi.org/10.1016/j.molstruc.2018.07.041>
47. Kurioz YI (2013) Phototransformations in cellulose cinnamate films at illumination with polarized UV light. *Ukr J Phys* 58:1138–1138. <https://doi.org/10.15407/ujpe58.12.1138>
48. Parka J, Grudniewski T, Kurioz Y, Dąbrowski R (2004) Liquid crystals with high photorefractive index and different cell construction solutions for optical light modulators. *Proc SPIE* 5565:321. <https://doi.org/10.1117/12.581204>

49. Morgan PW, Kwolek SL, Pletcher TC (1987) Aromatic azomethine polymers and fibers. *Macromolecules* 20:729–739. <https://doi.org/10.1021/ma00170a006>
50. Bléger D, Liebig T, Thiermann R, Maskos M, Rabe JP, Hecht S (2011) Light-orchestrated macromolecular “accordions”: reversible photoinduced shrinking of rigid-rod polymers. *Angew Chem* 123:12767–12771. <https://doi.org/10.1002/ange.201106879>
51. Robertus J, Reker S, Pijper T, Deuzeman A, Browne W, Feringa B (2012) Kinetic analysis of the thermal isomerisation pathways in an asymmetric double azobenzene switch. *Phys Chem Chem Phys* 14:4374–4382. <https://doi.org/10.1039/C2CP23756C>